BRAIN
ORIGINAL ARTICLE

SPTSSA variants alter sphingolipid synthesis and cause a complex hereditary spastic paraplegia

Siddharth Srivastava,[1,†] Hagar Mor Shaked,[2,†] Kenneth Gable,[3,†] Sita D. Gupta,[3,†]
Xueyang Pan,[4,5,†] Niranjanakumari Somashekarappa,[3] Gongshe Han,[3]
Payam Mohassel,[6] Marc Gotkine,[2] Elizabeth Doney,[7] Paula Goldenberg,[8]
Queenie K.-G. Tan,[9] Yi Gong,[10,11] Benjamin Kleinstiver,[11,12,13] Brian Wishart,[14]
Heidi Cope,[9] Claudia Brito Pires,[10,11] Hannah Stutzman,[11,12] Rebecca C. Spillmann,[9]
Undiagnosed Disease Network, Reza Sadjadi,[10] Orly Elpeleg,[2] Chia-Hsueh Lee,[15]
Hugo J. Bellen,[4,5] Simon Edvardson,[16] Florian Eichler[10,11,‡] and Teresa M. Dunn[3,‡]

[†,‡]These authors contributed equally to this work.

Sphingolipids are a diverse family of lipids with critical structural and signalling functions in the mammalian nervous system, where they are abundant in myelin membranes. Serine palmitoyltransferase, the enzyme that catalyses the rate-limiting reaction of sphingolipid synthesis, is composed of multiple subunits including an activating subunit, SPTSSA. Sphingolipids are both essential and cytotoxic and their synthesis must therefore be tightly regulated. Key to the homeostatic regulation are the ORMDL proteins that are bound to serine palmitoyltransferase and mediate feedback inhibition of enzymatic activity when sphingolipid levels become excessive.

Exome sequencing identified potential disease-causing variants in *SPTSSA* in three children presenting with a complex form of hereditary spastic paraplegia. The effect of these variants on the catalytic activity and homeostatic regulation of serine palmitoyltransferase was investigated in human embryonic kidney cells, patient fibroblasts and *Drosophila*.

Our results showed that two different pathogenic variants in *SPTSSA* caused a hereditary spastic paraplegia resulting in progressive motor disturbance with variable sensorineural hearing loss and language/cognitive dysfunction in three individuals. The variants in *SPTSSA* impaired the negative regulation of serine palmitoyltransferase by ORMDLs leading to excessive sphingolipid synthesis based on biochemical studies and *in vivo* studies in *Drosophila*.

These findings support the pathogenicity of the *SPTSSA* variants and point to excessive sphingolipid synthesis due to impaired homeostatic regulation of serine palmitoyltransferase as responsible for defects in early brain development and function.

1 Department of Neurology, Rosamund Stone Zander Translational Neuroscience Center, BostonChildren's Hospital, Harvard Medical School, Boston, MA 02115, USA
2 Department of Genetics, Hadassah Medical Center and Faculty of Medicine, Hebrew University of Jerusalem, Jerusalem 91120, Israel
3 Department of Biochemistry and Molecular Biology, Uniformed Services University of the Health Sciences, Bethesda, MD 20814, USA
4 Department of Molecular and Human Genetics, Baylor College of Medicine, Houston, TX 77030, USA
5 Jan and Dan Duncan Neurological Research Institute, Texas Children's Hospital, Houston, TX 77030, USA
6 Neuromuscular and Neurogenetic Disorders of Childhood Section, National Institute of Neurological Disorders and Stroke, National Institutes of Health, Bethesda, MD 20814, USA

7   Massachusetts Eye and Ear, Boston, MA 02114, USA
8   Department of Pediatrics, Section on Medical Genetics, Massachusetts General Hospital, Harvard Medical School, Boston, MA 02114, USA
9   Department of Pediatrics, Division of Medical Genetics, Duke University School of Medicine, Durham, NC 27710, USA
10 Department of Neurology, Massachusetts General Hospital, Harvard Medical School, Boston, MA 02114, USA
11 Center for Genomic Medicine, Massachusetts General Hospital, Harvard Medical School, Boston, MA 02114, USA
12 Department of Pathology, Massachusetts General Hospital, Boston, MA 02114, USA
13 Department of Pathology, Harvard Medical School, Boston, MA 02115, USA
14 Physical Medicine and Rehabilitation, Spaulding Rehabilitation Hospital, Harvard Medical School, Boston, MA 02114, USA
15 Department of Structural Biology, St. Jude Children's Research Hospital, Memphis, TN 38105, USA
16 Pediatric Neurology Unit, Hadassah University Hospital, Mount Scopus, Jerusalem 91240, Israel

Correspondence to: Teresa M. Dunn
Department of Biochemistry and Molecular Biology
Uniformed Services University of the Health Sciences
4301 Jones Bridge Road, Bethesda, MD 20814, USA
E-mail: teresa.dunn-giroux@usuhs.edu

Correspondence may also be addressed to: Florian S. Eichler
Center for Rare Neurological Diseases
Massachusetts General Hospital, Harvard Medical School
175 Cambridge Street, Suite 340, Boston, MA 02114, USA
E-mail: feichler@partners.org

Introduction

Sphingolipids (SLs) are crucial structural and functional components of membranes as well as potent signalling molecules.[1,2] Neurological disorders associated with lysosomal enzymes required for SL degradation have been known for decades and include Gaucher disease (GBA), Tay-Sachs disease (HEXA), Krabbe disease (GALC), Farber disease (ASAH1) and Niemann-Pick disease type A/B (SMPD1). More recently, disorders resulting from mutations in SL biosynthetic genes have been discovered. Such mutations affecting SL biosynthesis have been mostly linked to serine palmitoyltransferase (SPT).[3,4] SPT catalyses the initial step in SL biosynthesis, condensation of L-serine with an acyl-CoA to form a sphingoid or long-chain base (LCB) (Fig. 1A).[5–7] SPT activity is tightly regulated to ensure adequate SL synthesis while preventing excess, potentially toxic, SL accumulation.[8–10]

SPT is a multisubunit enzyme that resides in the endoplasmic reticulum (ER) membrane. The SPTLC1 (SPT long chain base subunit-1) subunit dimerizes with either SPTLC2 or SPTLC3 to form the active site. The SPTLC1/SPTLC2 and SPTLC1/SPTLC3 heterodimers have low basal catalytic activity that is stimulated >25-fold by either of two small proteins, SPTSSA (SPT small subunit A) or SPTSSB.[11] Recent cryogenic-electron microscopy (cryo-EM) studies revealed that SPT is a dimer of SPTLC1/SPTLC2/SPTSSA heterotrimers.[12–14] SPT is negatively regulated by ORMDL proteins, a family of three homologous and functionally redundant proteins that bind to and regulate SPT by feedback inhibition.[15–17] Cryo-EM structures of the tetrameric SPTLC1/SPTLC2/SPTSSA/ORMDL3 complex, similarly organized in a higher order dimer (Fig. 1B), have also been reported.[12–14] The presence of multiple SPT isozymes organized in higher order structures points to a previously unappreciated complexity in the committed step of SL synthesis.

Among the pathogenic variants in SPT that cause neurological disease are mutations in SPTLC1 and SPTLC2 that compromise amino acid substrate selectivity. Whereas wild-type (WT) SPT is highly selective for serine, SPT composed of the mutant SPTLC1 or SPTLC2 subunits also condenses alanine and glycine with palmitoyl-CoA to generate atypical deoxy-SLs associated with hereditary sensory neuropathy type 1 (HSAN1)[18–22] and macular telangiectasia type 2.[23] More recently, pathogenic variants in SPTLC1 causing childhood amyotrophic lateral sclerosis (ALS) were discovered.[10,24] These variants impair ORMDL-mediated feedback regulation of SPT causing excessive SL synthesis.[10]

Here, we report three individuals with disease-causing variants in SPTSSA, two with a de novo variant (p.Thr51Ile, SPTSSA^T51I) and one with a homozygous variant (p.Gln58AlafsTer10, SPTSSA^58fs). The individuals developed a complex form of hereditary spastic paraplegia (HSP) associated with progressive motor impairment and spasticity and variable language/cognitive impact. We investigated the functional impact of the SPTSSA variants on SL biosynthesis and its homeostatic regulation. Similar to the ALS-causing pathogenic variants in SPTLC1, the SPTSSA variants impaired ORMDL regulation and caused excessive SL synthesis. Excessive SL synthesis in a Drosophila model caused severe neurological defects and shortened lifespan. In summary, the data indicate that the SPTSSA variants are causative and provide a mechanistic understanding of the elevated SL synthesis that underlies progressive neurodegenerative disease.
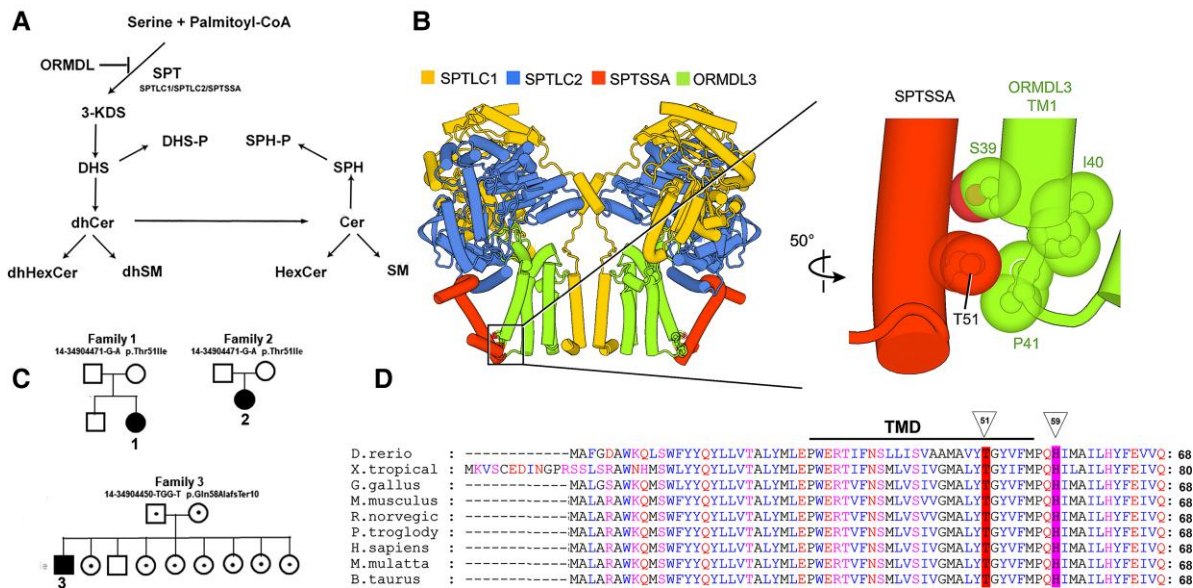
Figure 1 SL biosynthesis and HSP-causing variants in the SPTSSA subunit of SPT. (A) SPT catalyses the first and rate-limiting step of sphingolipid synthesis, the condensation of serine with an acyl-CoA (typically, palmitoyl-CoA) to generate the sphingoid base, 3-KDS, which is further modified to form the complex family of SLs. SPT is feedback inhibited by the ORMDL proteins. The dihydroceramide-based SLs [dihydroceramide (dhCer), dihydrohexosylceramide (dhHexCer) and dihydrosphingomyelin (dhSM)] do not usually accumulate to appreciable levels, but excessive SPT activity results in significant elevation of these SLs. **(B)** The SPT/ORMDL3 complex is a dimer of SPTLC1/SPTLC2/SPTSSA/ORMDL3 tetramers. The enlarged image (*right*) shows that Thr51 of SPTSSA is in close contact with the luminal end of the first (of four) transmembrane domain (TM1) of ORMDL3. **(C)** Pedigrees showing *de novo* occurrence of the heterozygous SPTSSA p.Thr51Ile variant in two families and the inherited p.Gln58AlafsTer10 variant in the third family. Filled symbols denote probands; dots in the centre of the circle or square denote carriers. **(D)** Thr51 (indicated by triangle) of the evolutionarily conserved SPTSSA subunit is located at the luminal end of the single transmembrane domain (TMD).

Materials and methods

Clinical studies

Research was performed in accordance with ethical standards of the responsible committees on human experimentation. Proper informed consent was obtained for all probands in this study. The Undiagnosed Disease Network (UDN) work, including clinical work, and coordination for this publication, was performed under NIH IRB protocol 15-HG-0130, MGH IRB Protocols 2012P000132 and 2007P002248, and the Duke University IRB protocol Pro00056651. The exome sequencing and the skin fibroblasts studies on Patient 3 were approved by the Hadassah Medical Center review board.

Plasmids

Plasmids for expression of SPTLC1 and SPTLC2 were purchased from OriGene. Plasmids for expressing NubG-HA-tagged SPTSSA and NubG-HA-tagged human ORMDL3 were described previously.[11,25] Variants in human SPTSSA were introduced by QuikChange mutagenesis (Agilent).

Antibodies

Antibodies for detecting SPTLC1 (BD Biosciences, #611304), SPTLC2 (Protein Tech 51012-2-ap), ORMDLs (EMD Millipore ABN417), GAPDH (Santa Cruz SC-47724), Calnexin (Santa Cruz SC-11397), HA (Anti-HA.11, BioLegend) and FLAG (Origene, #TA180144) were commercially available. The SPTSSA antibodies were generated by Vivitide using two peptides (MAGMALARAW KQC and CQHIMAILHYFEIVQ). Subsequent characterization revealed that the antibodies recognize only the C-terminal epitope of SPTSSA.

Cell culture and heavy serine labelling

Fibroblasts were obtained and expanded from patient skin biopsies according to published protocols.[26] The human embryonic kidney (HEK) 293 *SPTSSA* knockout (KO) cells were generated using a kit (KN409747, Origene). Cells were labelled with 3,3-D_2 L-serine (Cambridge Isotope Laboratories) as previously described.[10]

Drosophila stocks, maintenance and generation of human UAS-single chain SPT and UAS-ORMDL3 transgenic fly lines

Drosophila strains were cultured on standard food at 25°C. The *da-Gal4* (#5460), *Act-Gal4* (#4414), *elav-Gal4* (#458), *repo-Gal4* (#7415), *Mef2-Gal4* (#27390) and *SPARC-Gal4* (#77473) lines were obtained from the Bloomington Drosophila Stock Center (BDSC).

Human *UAS-scSPT* and *UAS-ORMDL3* lines were generated as described.[27] In brief, the human cDNA sequences were cloned into pGW-UAS-HA.attB vector[28] for injection into embryos and insertion into the VK37 (BDSC #24872) or VK33 (BDSC #24871) docking site by φC31 mediated transgenesis.[29] The human ORMDL3 clone (NM_139280.1) was from Ultimate ORF Clones (ThermoFisher). The SPT single-chain fusion cDNA clone was generated as described.[30] The SPTSSA T51I and H59L mutations were introduced into the single chain SPT (scSPT) using Q5 site-directed mutagenesis (NEB). A *UAS-Empty* line, generated by injecting pGW-UAS-HA.attB, was used as a control.

SPT assay

Microsomes were prepared from yeast, HEK cells and fibroblasts as previously described.[31] Reactions were initiated by adding 100 µg of

microsomal membrane to a reaction mix containing 50 mM HEPES, pH 8.1, 50 μM pyridoxal 5′-phosphate, 25 μM palmitoyl-CoA, 2.5 mM serine and 20 μCi of ^{3}H-serine. Where indicated, a BSA-C8-ceramide (Avanti) complex[32] was added. After 10 min, the reaction was processed as described.[31]

ORMDL siRNA transfection

HEK *SPTSSA* KO cells were transfected with plasmids expressing WT or mutant SPTSSAs along with 'Silencer' select siRNAs, *ORMDL1* (s41258), *ORMDL2* (s26474), and *ORMDL3* (s41260) or negative control siRNA (4390847) (ThermoFisher).

Immunoprecipitation and immunoblotting

Cells were lysed by sonication in 50 mM NaCl, 25 mM Tris-HCl pH 7.5, 1 mM EGTA, 10% glycerol, 0.3%, NP-40, 0.3% deoxycholate and 0.03% SDS with protease and phosphatase inhibitors (Sigma Aldrich). Proteins were resolved on NuPAGE Gels (NP0336, ThermoFisher) and transferred to nitrocellulose. For IPs, HEK *SPTSSA* KO cells co-expressing SPTLC1-Flag, SPTLC2 and either HA-tagged WT and untagged SPTSSA^{T51I} or untagged WT and HA-SPTSSA^{T51I} were collected, washed with PBS and lysed by sonication in 50 mM HEPES, pH 8.0, and 150 mM NaCl with protease inhibitors at 4°C. Following solubilization with 1% GDN for 2 h, samples were centrifuged at 22 000*g* for 45 min, anti-Flag beads (Sigma) were added to the supernatant and incubated overnight at 4°C. Following four washes with buffer containing 0.01% GDN and elution with 200 μg/ml Flag peptide, proteins were detected by immunoblotting using the Odyssey system (LI-COR).

Quantitative real-time PCR

RNA from fibroblasts was extracted with the *mir*Vana™ miRNA Isolation Kit (Invitrogen, AM1560) and cDNA was generated with the Applied Biosystems™ High-Capacity cDNA Reverse Transcription kit. RT-qPCR was conducted with TaqMan primers (SPTSSA, ID: Hs00370543_m1 or ACTB, ID: Hs01060665_g1) and the TaqMan™ Gene Expression Master Mix using the QuantStudio 6 Flex real time PCR system (ThermoFisher). The $2^{-\Delta\Delta CT}$ method[33] was used to calculate relative gene expression using actin as the internal control.

High performance liquid chromatography and mass spectrometry analysis

Two *Drosophila* larvae (late third instar) homogenized in TBS, serum (20 μl) or cell pellets (0.1–0.2 mg) were added to 1 ml methanol containing internal standards (Avanti, LM6002). Extraction, analysis and quantification of SLs by LCMS (liquid chromatography-mass spectrometry) were as described.[10]

Drosophila negative geotaxis climbing and lifespan assays

To measure negative geotaxis, flies were tapped to the bottom of a vial and their climbing distances were measured after 30 s. For the measurement of lifespan,[34] freshly eclosed flies were collected in separate vials and maintained at 25°C. Flies were transferred daily to fresh food for 6 days and every other day thereafter. Survival was determined during transfer. The results are presented as Kaplan–Meier curves.

Statistical analysis

Statistical analyses were carried out using the Student's unpaired two-tailed *t*-test for comparison of two groups. Multiple comparisons within the group were tested against the corresponding control. Kaplan–Meier survival curves were analysed using the Gehan–Breslow–Wilcoxon test and log-rank test. Calculated *P*-values of less than 0.05 were considered significant. All comparisons were significant (*P* < 0.05) unless noted as ns (not significant) in the figures. All statistical analyses were performed using GraphPad Prism, version 9.0.2 (GraphPad Software).

Data availability

The data that support the findings of this study are available from the corresponding author, upon reasonable request.

Results

Pathogenic SPTSSA variants lead to progressive motor dysfunction in children

Genetic analysis

Three individuals from three separate families with rare mutations in *SPTSSA* were identified through the Undiagnosed Disease Network (UDN) and international collaboration. Two of the affected individuals had the same *de novo* monoallelic variant and the third had an inherited biallelic variant. Genotype and clinical features are summarized in Fig. 1C and Table 1. Patients 1 and 2 both had a heterozygous *de novo* SPTSSA^{T51I} variant, absent from the population databases. The Thr51 residue of SPTSSA is highly conserved (Fig. 1D) and *in silico* analysis [PolyPhen-2 score of 0.999 (http://genetics.bwh.harvard.edu/pph2/index.shtml)] indicates that its substitution with isoleucine is likely to be protein damaging. Patient 3 harboured a homozygous frameshift variant, SPTSSA^{58fs}. This 2-nucleotide deletion, in the second (of two) exon of *SPTSSA*, is predicted to result in substitution of the C-terminal 14 amino acids with 10 out-of-frame amino acids. This variant has a minor allele frequency of 0.0000517 in the general population but a much higher frequency (0.001191) in the Ashkenazi Jewish population. It has not previously been observed in the homozygous state (https://gnomad.broadinstitute.org/gene/ENSG00000165389?dataset=gnomad_r2_1). *In silico* analyses (gnomAD) indicate that it is a low confidence loss-of-function allele.

Clinical features of affected patients

Patient 1 is currently 5 years old. Perinatal history was unremarkable. A port wine stain was present at birth (Supplementary Fig. 1), but workup for Sturge Weber syndrome and other vascular anomalies was negative. Her developmental profile is consistent with progressive lower extremity spasticity and cognitive delay. In terms of motor skills, she started sitting around 11 months. She underwent surgery for release of a tethered cord at 20 months of age. By 3 years of age, she had a scissoring gait and used a walker. In terms of language skills, she started babbling at 12 months. At the age of 25 months, she could use 15 words and signed two-word phrases. By 4 years of age, she could use 4–6-word phrases but had evidence of sensorineural hearing loss. Brain MRI performed at 1 year of age showed mild ventriculomegaly with slightly depressed white matter volume (corpus callosal thickness near the 3rd percentile for age). Electroencephalography at 2 years of age showed frequent sleep

Table 1 Genetic and clinical features associated with SPTSSA related disorder

	Patient 1 (Female)	Patient 2 (Female)	Patient 3 (Male)
Genetics			
Method of variant detection	Exome sequencing	Whole genome sequencing	Exome sequencing
cDNA change	NM_138288.3: c.152C>T	NM_138288.3: c.152C>T	NM_138288.3: c.171_172del
Protein change	p.(Thr51Ile)	p.(Thr51Ile)	p.(Gln58AlafsTer10)
Inheritance	*De novo*	*De novo*	Autosomal recessive
Heterozygosity	Heterozygous	Heterozygous	Homozygous
Growth features			
Failure to thrive	No	Yes	Yes
Short stature	Yes	Yes	Yes
Macrocephaly	Yes	No	No
Weight (CDC z-score)	Age 50 mo: 12.7 kg (−1.99)	Age 8 y: 17.7 kg (−2.42)	Age 22 y: 50 kg
Height (CDC z-score)	Age 50 mo: 85.5 cm (−3.76)	Age 8 y: 111.5 cm (−2.87)	Age 22 y: 145 cm
Head circumference (CDC z-score)	Age 28 mo: 49.5 cm (1.14)	Age 8 y: 50 cm (−1.31)	Age 13 y: 53 cm
Birth weight (CDC z-score)	2.8 kg (−1.19)	3.6 kg (0.44)	3.25 kg
Birth length (CDC z-score)	50.8 cm (0.49)	53.3 cm (1.40)	
Development			
Intellectual disability	No	Yes	No
Age babbling	12 mo	12 mo	10 mo
Age first word besides mama/dada	30 mo	No words	12 mo
Age phrases	Five-word phrases at 3 y		Two-word phrases at 2 y
Current best language abilities	Age 4 y: 4–6-word phrases	Age 8 y: no words/gestures; communicates with facial/eye expressions and voice tone	Normal
Age sitting	12–14 mo	Not sitting	
Age walking	2 y: 10–15 steps with walker	Not walking	24 mo
Current best motor functioning	Scissoring gait using walker	Holds head up briefly	Stands supported
Neurological features			
Axial hypotonia	Yes	Yes	No
Appendicular spasticity	Yes	Yes	Yes
Dystonia	No	Suspected	No
Gait pattern	Spastic gait	Not walking	Not walking
Cortical visual impairment	No	Suspected	No
Epilepsy	No	No	Yes (rolandic)
EEG findings	Frequent sleep potentiated multifocal spikes involving left central, left frontal, right centro-parietal, right frontal regions, rarely synchronized	Mild diffuse background slowing with overriding diffuse beta range frequency; multifocal polymorphic sharp waves and sharp slow waves during sleep, most frequent bi-temporal independent	Temporoparietal spikes
Disrupted sleep	No	Yes	No
Dysphagia	No	Yes	No
Sialorrhea	No	Yes (requiring botox and scopolamine)	No
Sensorineural hearing loss	Yes	No	Yes
Autonomic instability	No	Yes (temperature instability)	No
Tethered cord	Yes	No	No
Systemic features			
Ophthalmological features	None	None	Myopia
ENT features	None	Type 1 laryngeal cleft	None
Gastrointestinal features	GERD	GERD, constipation, G-tube	None
Renal features	None	Renal tubular acidosis and nephrolithiasis (requiring ureteral stents, lithotripsy); UTI	None
Musculoskeletal features	None	Severe levoscoliosis, bilateral proximal femoral osteotomies	Tendon releases and osteotomies for contractures
Endocrine features	Growth hormone deficiency		
Dermatological features	Capillary malformation on forehead, upper eyelids, nape of neck/back of head and lower part of spine	Nevus flammeus on central forehead extending over both eyelids; stork bite nape of neck	None

GERD = gastroesophageal reflux disorder; mo = months; UTI = urinary tract infections; y = years.

potentiated multifocal spikes which rarely synchronized but no evidence of clinical seizures. Nerve conduction studies (NCS) at 3 years of age showed no signs of polyneuropathy. Her neurological examination at 46 months of age was notable for central hypotonia, lower extremity spasticity (worsened over time without proximal or distal preference), a positive Babinski sign and an abnormal gait pattern (scissoring, extreme toe walking, and inversion of the feet).

Patient 2 is currently 10 years old. She was born at 39 weeks gestation after an uneventful pregnancy. A port wine stain was apparent in infancy. Her developmental trajectory is characterized by progressive spasticity (lower > upper), possible dystonia and intellectual disability (ID). Motor delay was noted at 5 months of age. At 8 years of age, she had no control of her legs and some control of her arms. By 10 years of age, spasticity was worse in the lower extremities but also present in the upper extremities, with clonus at the wrists bilaterally. She could not hold her head up consistently and never acquired the ability to sit independently or reach for objects. Worsening spasticity led to hip displacement, and poor truncal tone contributed to severe scoliosis. In terms of language, at the age of 8 years, she was non-verbal and communicated with facial/eye expressions and tone of voice. This degree of communication impairment, in combination with significantly impaired adaptive skills, was consistent with ID. At 15 months of age, she developed staring spells and episodes of body stiffening, neither of which were associated with epileptiform activity on EEG. Her EEG showed mild diffuse background slowing, multifocal polymorphic sharp waves, and sharp slow waves during sleep, but no seizures. Electromyography (EMG)/NCS showed no evidence of polyneuropathy or motor neuron disease. Brain MRI at 2 years of age showed ventriculomegaly and abnormal T_2 hyperintensity in the deep and periventricular white matter bilaterally. Magnetic resonance spectroscopy of both grey matter (caudate) and white matter (parietal-occipital) voxels showed decreased N-acetylaspartate (NAA) and increased lactate signals. A repeat brain MRI at 4 years of age showed progressive cerebral volume loss and development of cerebellar atrophy. Her current neurological examination shows truncal hypotonia, spasticity in all extremities, and hyperreflexia. Beyond her neurological impairment, she also had systemic complications and comorbidities. Due to dysphagia, reflux, frequent vomiting and recurrent aspiration pneumonias, she underwent placement of a gastrostomy tube at 2 years of age. Over time, she also developed renal tubular acidosis and nephrolithiasis.

Patient 3, currently 22 years old, is the second child out of nine to non-consanguineous Jewish Ashkenazi parents. He was born at term after an uneventful pregnancy. His neurodevelopmental profile is characterized by regression in motor skills, progressive spasticity and weakness. Early motor development was delayed, as he walked independently at 2 years of age. At 7 years of age, contractures in the lower limbs prompted surgery for tendon release at multiple levels. At 10 years of age, he developed motor regression, losing the ability to walk. Pyramidal signs with appendicular spasticity and hyperreflexia led to an initial diagnosis of cerebral palsy. Sensorineural hearing loss was diagnosed at 3 years of age, and the initial speech delay gradually improved after use of hearing aids. No further deterioration of hearing has occurred. In addition to developmental impairment, he had seizures. Around 6 years of age, he developed rolandic seizures with temporoparietal spike-waves evident on EEG. By 12 years of age, the seizures abated having required no treatment. A brain MRI at the time showed mild thinning of the corpus callosum. NCS showed no signs of polyneuropathy. On examination at 22 years of age, he displayed weakness, spasticity and hyperreflexia, more prominent in the legs than in the arms.

In summary, all three individuals presented with progressive motor impairment (Table 1). Neurological impairment ranged from severe (inability to sit unsupported and lack of verbal communication up until 10 years of age in Patient 2) to moderate (ability to ambulate until 10 years of age and preserved verbal communication beyond 20 years of age in Patient 3). All patients showed an early period of developmental delay and progressive spasticity, predominantly in the lower extremities. While EEG abnormalities were present in all three patients, clinical seizures manifested in only one and required no intervention. Both sensorineural hearing loss and a port-wine stain were features present in 2 of 3 subjects (Fig. 2C and Supplementary Fig. 1, respectively). NCS showed no evidence of polyneuropathy or lower motor neuron disease. Brain MRIs showed varying degrees of cerebral volume loss and cerebellar atrophy (Fig. 2A). Magnetic resonance spectroscopy in one patient (Patient 2) demonstrated decreased NAA and increased lactate signals (Fig. 2A). Serum levels of SLs were increased in all three patients (Fig. 4A) and prompted further exploration in HEK cells, patient fibroblasts and *Drosophila* as described below.

The SPTSSA[58fs] variant, but not the SPTSSA[T51I] variant, reduces microsomal SPT activity

Although homozygous *Sptssa* KO mice are inviable, heterozygous *Sptssa* null mutant mice develop normally.[35] Thus, it is unlikely that the *de novo* SPTSSA[T51I] variant is a simple loss-of-function mutation that prevents activation of the SPTLC1/SPTLC2 heterodimer. The Genome Aggregation Database (gnomAD) suggests *SPTSSA* is tolerant of heterozygous loss-of-function variants predicted to result in haploinsufficiency.[36]

To directly test whether the T51I mutation in SPTSSA altered its activation of SPT, SPT activity was measured in microsomes prepared from HEK *SPTSSA* KO cells expressing either WT SPTSSA or SPTSSA[T51I]. Microsomal SPT activity from the *SPTSSA* KO cells was near the limit of detection (~1 pmol/mg/min) whereas SPT activity from cells expressing WT SPTSSA was ~30 pmol/mg/min (Fig. 3A), consistent with our previous reports that the SPTLC1/SPTLC2 heterodimer is activated >25-fold by SPTSSA.[11,31] SPTSSA[T51I] activated the SPTLC1/SPTLC2 heterodimer comparably to WT SPTSSA (Fig. 3A), and immunoblotting showed that it was expressed similarly to WT SPTSSA (Fig. 3B). Furthermore, co-immunoprecipitation with SPTLC1-Flag showed that SPTSSA[T51I] bound the SPTLC1/SPTLC2 heterodimer comparably to WT SPTSSA (Fig. 3C). Microsomal SPT activity measured from the patient fibroblasts was also comparable to that from age and gender matched control fibroblasts (Fig. 3D). Overall, these results demonstrated that the T51I variant in *SPTSSA* did not alter the intrinsic enzymatic activity of SPTLC1/SPTLC2/SPTSSA heterotrimeric SPT and thus that the SPTSSA[T51I] subunit is a completely functional activator of the SPTLC1/SPTLC2 heterodimer.

We also investigated whether the SPTSSA[58fs] variant impacted the activation of SPT. In contrast to SPTSSA[T51I], which is a *de novo* dominant variant, SPTSSA[58fs] was inherited in an autosomal recessive manner. Both unaffected parents and seven unaffected siblings of the proband were carriers of the SPTSSA[58fs] allele (Fig. 1C). Given the importance of SPT activity, it seemed possible that this mutation compromises the activating function of SPTSSA, thereby resulting in insufficient SL synthesis. To test this idea, microsomal SPT activities from fibroblasts of the patient, unaffected carrier mother and homozygous WT brother were compared. The results showed that SPT activity was significantly lower in microsomes from the SPTSSA[58fs] patient fibroblasts
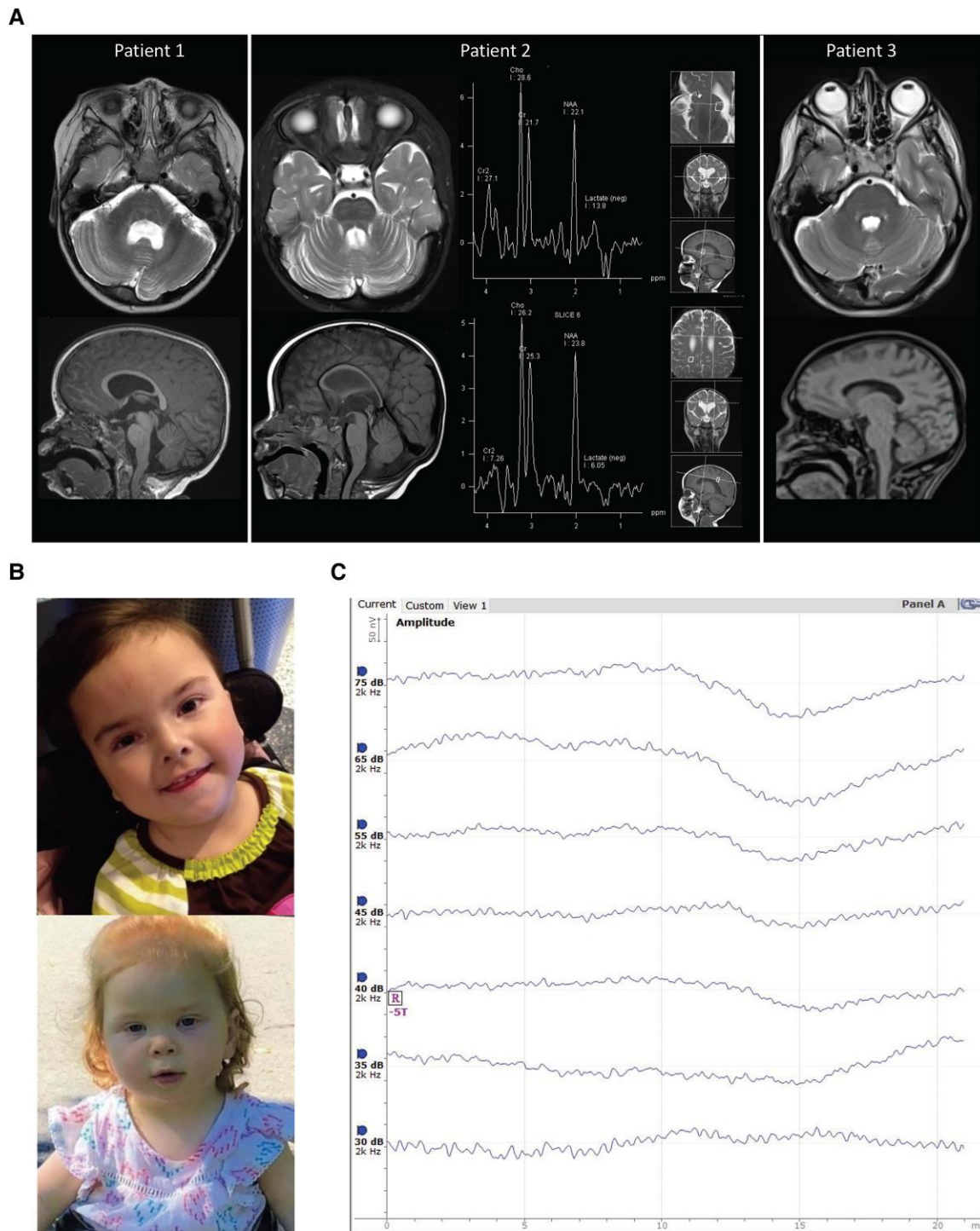
Figure 2 Clinical characteristics of patients with SPTSSA-related disorder. (A) Variable findings on brain MRI among affected individuals with SPTSSA variants, including cerebral/cerebellar volume loss and white matter changes. Axial and sagittal images shown are from Patient 1, who has ventriculomegaly and slightly depressed white matter volume. In Patient 2, at age 2 years, magnetic resonance spectroscopy of both grey (caudate) and white (parietal-occipital) matter voxels showed decreased NAA and increased lactate signals. At age 4 years, there was interval development of cerebellar atrophy and mild progressive cerebral volume loss with T_2 hyperintensity in the deep and periventricular white matter bilaterally. In Patient 3, scans at age 12 years showed mild thinning of the corpus callosum but structures were within the normal range. **(B)** Facial dysmorphisms of affected individuals with the SPTSSA p.Thr51Ile variant. **(C)** Threshold BAER (brainstem auditory evoked response) evaluation showed elevated thresholds for hearing, as determined by presence/absence of wave V when measured using a 2 kHz tone burst at various stimulation levels, in Patient 1. Shown is response from the left ear with a threshold of 35 dBnHL (decibels normal hearing level).

(Fig. 3E). It was not possible to compare expression of the WT SPTSSA and SPTSSA[58fs] subunits in fibroblasts by immunoblotting, because the SPTSSA antibody recognizes the C-terminus of SPTSSA, which is missing from the mutant subunit. However, HA-tagged SPTSSA[58fs] expressed poorly compared to HA-tagged WT in the HEK *SPTSSA* KO cells (Fig. 3B). Reduced expression of the mutant SPTSSA subunit likely accounted for reduced SPT activity in the patient fibroblasts and may also have explained why microsomal SPT activity was not compromised in the carrier mother's fibroblasts, since the majority of her SPT presumably contained the more highly expressed WT SPTSSA. The observation that SPTSSA[58fs] expression from a cDNA (Fig. 3B) was low pointed to reduced stability of the protein but did not rule out the possibility that the frameshift variant also affected mRNA stability. To address this, RT-qPCR was conducted and showed no significant difference in SPTSSA mRNA levels in fibroblasts from Patient 3 (homozygous for the frameshift variant) and his unaffected brother (homozygous WT) (Supplementary Fig. 2A). In addition, cDNA from the mother's fibroblasts was used to make an SPTSSA amplicon and sequencing of 24 clonally purified plasmids showed that the WT and 58fs variants were equally represented in the mother's mRNA (Supplementary Fig. 2B). Despite the reduced stability of the SPTSSA[58fs] protein, SPT activity was comparable in microsomes from the HEK *SPTSSA* KO cells expressing the mutant and WT SPTSSA (Fig. 3A), indicating that, when expressed at sufficient levels, SPTSSA[58fs] fully activates the SPTLC1/SPTLC2 heterodimer.

Both SPTSSA variants increase intracellular SPT activity

Although microsomal SPT activity was not affected by the SPTSSA[T51I] variant (Fig. 3A and D), levels of several SLs were substantially elevated in serum from the SPTSSA[T51I] patients compared to controls (Fig. 4A). Since the rate of intracellular SL synthesis reflects both the intrinsic catalytic activity of SPT as well as its homeostatic regulation, these results raised the possibility that the T51I mutation in SPTSSA interferes with the negative feedback regulation of SPT.

To investigate this idea further, SPT activity was compared in HEK *SPTSSA* KO cells expressing the T51I mutant or WT SPTSSA subunit. As expected, intracellular SPT activity, determined by measuring incorporation of d2-serine into newly synthesized SLs, was very low in the *SPTSSA* KO cells and significantly increased by expression of SPTSSA (Fig. 4B). Strikingly, expression of SPTSSA[T51I] led to much higher intracellular SPT activity than did expression of WT SPTSSA (Fig. 4C). The same result was seen when *de novo* SL synthesis in patient and control fibroblasts was compared (Fig. 4D).

Surprisingly, although the SPTSSA[58fs] mutant subunit was poorly expressed and microsomal SPT activity in the patient fibroblasts was low (Fig. 3E), SL levels were also elevated in serum from Patient 3 (Fig. 4A). Likewise, intracellular SPT activity was significantly higher in HEK *SPTSSA* KO cells expressing SPTSSA[58fs] than in cells expressing WT SPTSSA (Fig. 4C). More importantly, *de novo* SL synthesis in the patient fibroblasts was substantially higher than in fibroblasts from the mother or unaffected brother (Fig. 4E). Thus, although the SPTSSA[58fs] frameshift variant reduced expression of SPTSSA, it nonetheless resulted in elevated intracellular SPT activity.

The SPTSSA variants impair ORMDL-mediated inhibition of SPT

The increased SPT activity observed in cells expressing the SPTSSA variants suggested that ORMDL-mediated regulation of SPT may be impaired by the mutations, given that the ORMDL proteins inhibit

SPT when SL levels become too high. In support of this notion, for the SPTSSA[T51I] variant, the cryo-EM structure of the human SPT/ORMDL3 complex[12,13] reveals that T51, highly conserved among eukaryotes (Fig. 1D), resides at the luminal end of the single transmembrane domain of SPTSSA in close association with the first transmembrane domain (TM1) of ORMDL3 (Fig. 1B). It is less clear how the 58fs variant might affect interactions with ORMDL because this domain of SPTSSA is not visible in the cryo-EM structures.[12,13]

Several lines of evidence indicated that SPTSSA[T51I]-containing SPT was indeed refractory to ORMDL regulation. First, SPTLC1, SPTLC2, and either WT or SPTSSA[T51I] were overexpressed in HEK cells. By overexpressing SPT, the regulatory capacity of the endogenous ORMDLs was exceeded and thus the ability of co-transfected ORMDL3 to regulate SPT activity could be assessed by measuring incorporation of d2-serine into newly synthesized SLs (Fig. 1A).[25] The results showed that SPT containing SPTSSA[T51I] was less responsive to inhibition by co-transfected ORMDL3 than SPT containing WT SPTSSA (Fig. 5A and Supplementary Fig. 3A). Another indicator of ORMDL regulation is the ability of cells to maintain SL levels when serine is added to the growth media. Although increased serine concentrations increase SPT activity, the accumulating SLs invoke ORMDL-mediated inhibition of SPT to maintain SL homeostasis.[10] Accordingly, *de novo* SL synthesis was largely unaffected by increased serine in HEK *SPTSSA* KO cells expressing WT SPTSSA. By contrast, it was markedly elevated in these cells expressing the SPTSSA[T51I] mutant subunit (Fig. 5B), further indicating that the T51I mutation abrogated ORMDL regulation. It has also been shown that C8-ceramide represses microsomal SPT activity in an ORMDL-dependent manner.[32] As predicted, microsomal SPT from the patient fibroblasts was less responsive to ORMDL-dependent C8-ceramide inhibition than microsomal SPT activity from control fibroblasts (Fig. 5C), again pointing to loss of ORMDL regulation. Finally, the consequences of silencing the ORMDLs in HEK *SPTSSA* KO cells expressing the WT or T51I mutant SPTSSA was compared. Similar to previous reports,[15,37,38] silencing the ORMDLs increased *de novo* SL synthesis several-fold in cells expressing WT SPTSSA; however, it had little effect on *de novo* SL synthesis in cells expressing SPTSSA[T51I] (Fig. 5D). Taken together, these results showed reduced ORMDL regulation of SPT containing the SPTSSA[T51I] mutant subunit and strongly implicated unrestrained SPT activity as the underlying cause of the pathophysiology associated with the SPTSSA[T51I] variant. Since SPTSSA[T51I] expresses and binds SPTLC1/SPTLC2 analogously to WT SPTSSA (Fig. 3B and C), it is presumed that at least 50% of the patient's cellular SPT is not properly feedback inhibited by the ORMDLs. Thus, the T51I substitution in SPTSSA is a dominant loss-of-function mutation with regard to ORMDL regulation.

Similar to SPT composed of the SPTSSA[T51I] mutant subunit, SPT containing the SPTSSA[58fs] variant subunit was also less responsive to co-transfected ORMDL than WT SPT (Fig. 5A). In addition, as was observed for SPT containing SPTSSA[T51I], SPT containing SPTSSA[58fs] was impaired in the ORMDL-mediated homeostatic regulation elicited by increased serine (Fig. 5B). Finally, although silencing the ORMDLs increased intracellular SPT activity in the *SPTSSA* KO cells expressing SPTSSA[58fs], the increase was significantly smaller than in cells expressing WT SPTSSA (Fig. 5D). Taken together, the results showed that the SPTSSA[58fs] variant also significantly abrogated ORMDL regulation of SPT, albeit less so than the T51I mutation. Thus, although the SPTSSA[58fs] mutation reduced the stability of SPTSSA, intracellular SPT activity was, in fact, high and unregulated pointing to excessive rather than insufficient SLs as the basis of the pathophysiology in the patient. That this variant was
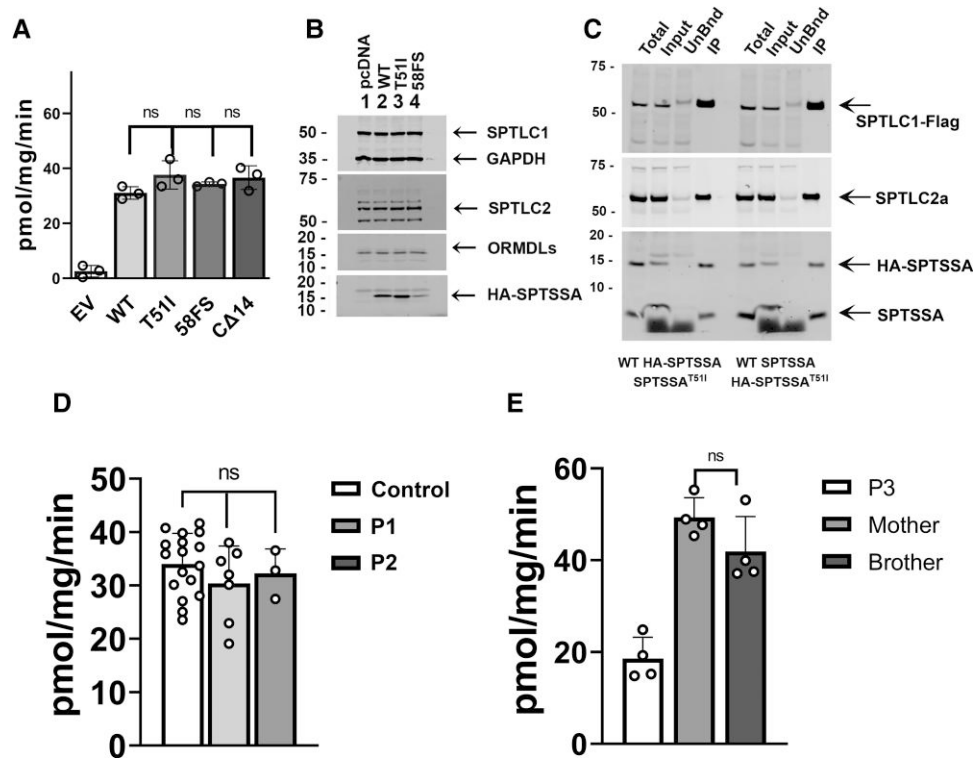
Figure 3 Effect of the *SPTSSA* variants on expression and activation of the SPTLC1/SPTLC2 heterodimer. (A) Plasmids expressing HA-tagged WT, SPTSSA[T51I] (T51I), SPTSSA[58fs] (58FS) or SPTSSA[CΔ14] (C[Δ14]) were transfected into HEK *SPTSSA* KO cells, and microsomal SPT activity was determined as described in the 'Materials and methods' section. **(B)** Microsomal proteins from the HEK *SPTSSA* KO cells expressing the indicated SPTSSA variants (as in **A**) were separated by SDS PAGE, and the indicated proteins were analysed by immunoblotting. **(C)** Microsomes prepared from *SPTSSA* KO cells co-expressing SPTLC1-FLAG, SPTLC2 and either HA-SPTSSA and SPTSSA[T51I] (*left*) or SPTSSA and HA-SPTSSA[T51I] (*right*) were solubilized and bound to anti-FLAG beads. The immunoprecipitated proteins were analysed by immunoblotting. **(D)** Microsomes prepared from Patients 1 and 2 (P1 and P2) and age-matched control (Con) fibroblasts were assayed for SPT activity as in **A**. **(E)** SPT activity in microsomes from Patient 3 (P3), his carrier mother and his homozygous WT brother was determined as in **A**.

recessive likely reflected both instability of the mutant SPTSSA (i.e. the majority of SPT in heterozygotes presumably contained WT SPTSSA) and that this variant impaired ORMDL regulation less than did the T51I variant.

The observation that the SPTSSA[58fs] mutation impairs ORMDL regulation of SPT suggested the C-terminus of SPTSSA plays a critical role in ORMDL-mediated inhibition of SPT. Indeed, we found that deletion of the C-terminal 14 amino acids of SPTSSA (SPTSSA[CΔ14]) did not affect ability to activate the SPTLC1/SPTLC2 heterodimer (Fig. 3A), but significantly impacted the response to ORMDL3 (Supplementary Fig. 3A). Furthermore, silencing the ORMDLs had a much smaller effect on SL levels in cells expressing SPTSSA[CΔ14] than on cells expressing WT SPTSSA (Supplementary Fig. 3B). These results prompted us to consider whether the SPTSSB[H56L] mutation, which resulted in high SLs and a neurodegenerative phenotype in the *stellar* mouse,[39] might also be disrupting ORMDL regulation. This residue is highly conserved between the SPTSSA and SPTSSB, being His59 in SPTSSA (Fig. 1D). Thus, we investigated the SPTSSA[H59L] variant and found that it also impaired ORMDL regulation (Supplementary Fig. 3A).

Increased SPT activity causes neurological defects in *Drosophila*

SPT is highly conserved in eukaryotes and *Drosophila melanogaster* is a powerful model for studying SL metabolism and human genetic disorders.[40,41] *Drosophila* produces sphingoid bases of different

chain lengths (C14/16)[42] from human (predominantly C18), allowing us to test the effect of the *SPTSSA* variants on human SPT activity by measuring C18 SLs. To determine the effect of increased SPT activity *in vivo*, we overexpressed the three human SPT subunits in *Drosophila* using a scSPT (Fig. 6A).[32] We used a variety of GAL4 drivers to express WT *scSPT* (*scSPT[Ref]*) in all cells or in various tissues. Ubiquitous *scSPT[Ref]* expression using either the comparatively weak *da-Gal4* or stronger *Act-Gal4* driver caused lethality (Table 2), showing that *scSPT* overexpression was toxic. The *Act>scSPT[Ref]* animals died at various developmental stages while all *da>scSPT[Ref]* animals died at late pupal stage, indicating that stronger *scSPT* expression caused more severe defects. We then overexpressed *scSPT* in the nervous system using pan-neuronal *elav-Gal4* and glial *repo-Gal4* drivers. The *elav>scSPT[Ref]* animals survived into adulthood but showed severely compromised climbing activity and a very short lifespan (Fig. 6B, C and E). Surprisingly, *scSPT[Ref]* expression in glial cells, which comprise only 10% of the cells of the nervous system, was sufficient to cause lethality (Table 2), indicating that glial cells were very sensitive to *scSPT* overexpression. Overexpression of *scSPT* in muscle (*Mef2-Gal4*) and fat body (*SPARC-Gal4*) also caused lethality (Table 2), showing that *scSPT* overexpression was toxic in most tissues.

Next we sought to study the impact of SPTSSA variants on SPT function. Because of the difficulty with testing the *SPTSSA* frameshift variant in the scSPT, we only tested the missense variant by introducing the SPTSSA[T51I] mutation into *scSPT* (*scSPT[T51I]*). In addition to the patient variant, we also tested the H59L missense
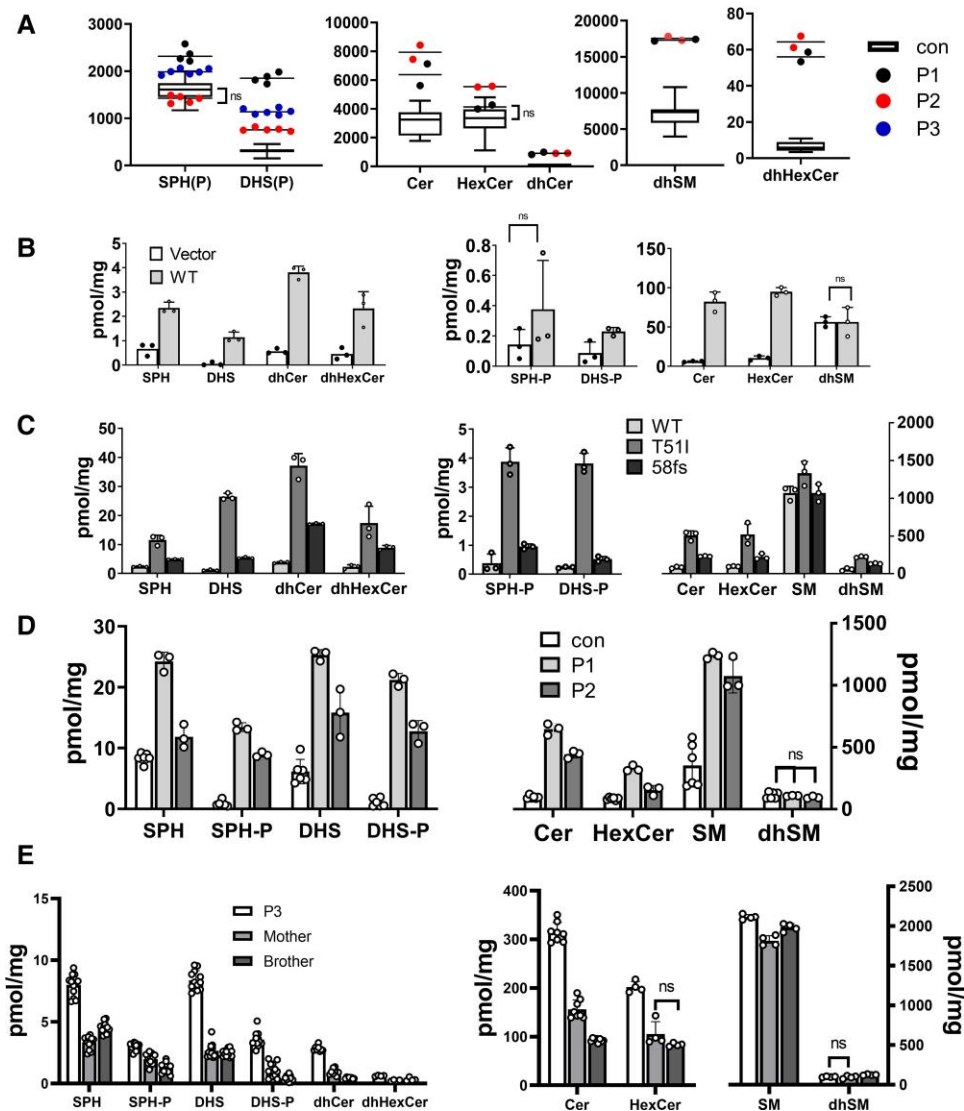
Figure 4 The *SPTSSA* variants increase SPT activity. (**A**) SLs were extracted from serum of patients (P1, P2 and P3) and 14 unaffected controls (Con) and the indicated SL species were quantified by LCMS as described in the 'Materials and methods' section. (**B**) HEK *SPTSSA* KO cells were transfected with a plasmid expressing WT SPTSSA or empty vector and after 24 h fresh medium containing d2-serine was added; 24 h later newly synthesized d2-labelled SLs were quantitated by LCMS. (**C**) Plasmids expressing WT, p.Thr51Ile (T51I), or p.Gln58AlafsTer10 (58fs) SPTSSA were transfected into the HEK *SPTSSA* KO cells and de novo SL synthesis was analysed as in **B**. (**D**) Patient P1 and P2 and control (Con) fibroblasts were incubated for 24 h in medium containing d2-serine, and labelled SLs were quantitated by LCMS as in **B**. (**E**) Fibroblasts from Patient 3 (P3), his carrier mother and his homozygous WT brother were incubated with d2-serine and SLs were extracted and quantitated as in **D**. Unless indicated as not significant (ns), all differences were significant (P < 0.05).

variant which is analogous to the mouse *Sptssb* p.H56L variant that caused elevated SL synthesis and neurodegeneration in the *stellar* mice[39] (discussed above). Flies expressing *scSPT*[T51I] or *scSPT*[H59L] are lethal or exhibit a very reduced lifespan similar to the *da>scSPT*[Ref] and *elav>scSPT*[Ref] flies, respectively (Table 2, Fig. 6B and Supplementary Fig. 4A and B), indicating that the SPTSSA T51I and H59L variants are not impairing SL synthesis.

Given that the previous data indicated that the T51I variant acts as gain-of-function because the ORMDL regulation is impaired, we explored the impact of co-expressing *scSPT* and *ORMDL3*. As shown in Table 2, *ORMDL3* expression fully rescued the phenotypes caused by *scSPT*[Ref] overexpression using various GAL4 drivers. However, co-expression of *ORMDL3* failed to rescue the motor defects and short lifespan in *elav>scSPT*[T51I] flies (Fig. 6B and D). Although *ORMDL3* expression rescued the lethality of the

da>ORMDL3, scSPT[T51I] flies, the surviving adults exhibited motor defects and a very short lifespan similar to the *elav>scSPT*[Ref] and the *elav>scSPT*[T51I] flies (Fig. 6C and E. These results showed that the *SPTSSA*[T51I] variant is a gain-of-function variant that disrupts the negative ORMDL regulation of SPT activity in vivo and that the inhibition of SL synthesis can be recapitulated in flies. Co-expression of *ORMDL3* also rescued the lethality of the *da>ORMDL3, scSPT*[H59L] flies (Supplementary Fig. 4A) but only partially rescued the motor defects caused by *da>scSPT*[H59L] and *elav>scSPT*[H59L] (Supplementary Fig. 4B). These data show that the H59L variant disrupts ORMDL regulation of SPT activity albeit to a lesser extent than the T51I variant. These results, together with the results from the 58fs variant and the C-terminal deletion mutant, indicate an important role for the C-terminus of SPTSSA in ORMDL regulation.
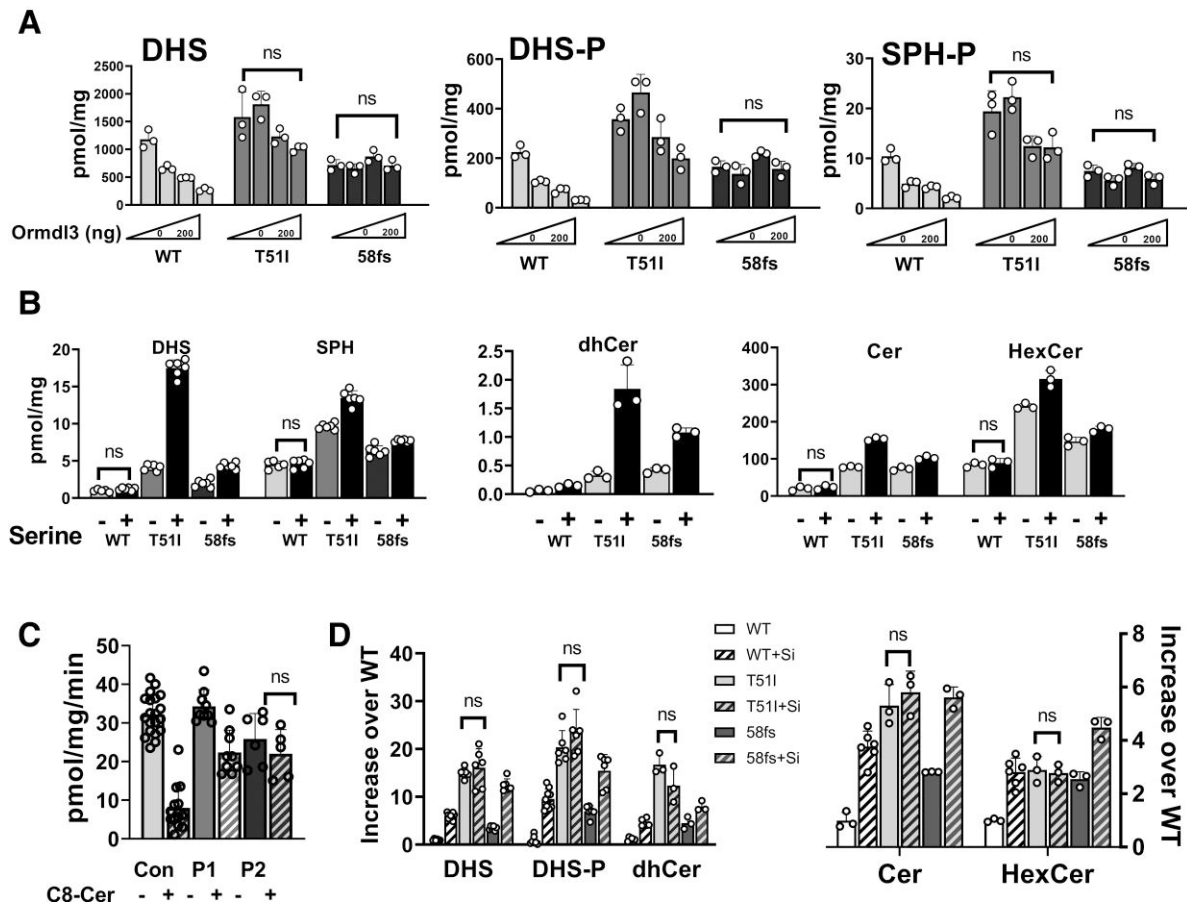
Figure 5 The *SPTSSA* variants impair ORMDL-mediated inhibition of SPT. (**A**) Plasmids expressing SPTLC1, SPTLC2 and WT, p.Thr51Ile (T51I), or p.Gln58AlafsTer10 (58fs) SPTSSA were transfected into HEK cells along with increasing amounts (0, 50, 100 or 200 ng) of ORMDL3-expressing plasmid. After 16 h, d2-serine was added, and 24 h later cells were harvested and deuterated SLs were quantitated by LCMS. (**B**) HEK *SPTSSA* KO cells were transfected with plasmids expressing WT, p.Thr51Ile (T51I), or p.Gln58AlafsTer10 (58fs) SPTSSA. After 24 h, fresh medium without (−) or with (+) 3 mM serine was added, and 24 h later cells were harvested for SL analyses by LCMS. (**C**) Microsomes prepared from patient (P1, P2) and control (Con) fibroblasts were assayed for SPT activity without (−) or with (+) added C8-ceramide(Cer)/BSA as described in the 'Materials and methods' section. (**D**) HEK *SPTSSA* KO cells were transfected with plasmids expressing WT, p.Thr51Ile (T51I) or p.Gln58AlafsTer10 (58fs) SPTSSA and SiRNAs (+Si) directed to ORMDL1, 2 and 3 or a control scrambled siRNA. After 24 h, the medium was changed, d2-serine was added for 24 h, cells were harvested and deuterated SLs were quantitated by LCMS. Unless indicated as not significant (ns), all differences were significant ($P < 0.05$).

To confirm that the *scSPT* overexpression phenotypes are caused by elevated SL synthesis, we measured SL levels in fly larvae. *Drosophila* SPT produces SLs with C14 and C16 LCBs,[42] while human SPT produces SLs with C18 LCBs. We found that the C14 and C16 LCB levels were not significantly elevated when *scSPT* was overexpressed whereas the *da>Empty* control and the *da>ORMDL3* larvae did not produce C18 SLs (Fig. 6F). However, both *da>scSPT*[Ref] larvae and the *da>scSPT*[T51I] larvae had elevated levels of total C18 LCBs (Fig. 6F) as well as C18 ceramide and C18 ceramide phosphoethanolamine (CPE), two commonly observed complex SLs in *Drosophila* (Fig. 6G). Hence, expression of the human *scSPT* was sufficient to induce the production of C18 SLs in flies. Importantly, co-expression of *ORMDL3* abolished the C18 SL levels, showing that the regulation of human SPT by ORMDL3 can be fully recapitulated in flies. Consistent with the behavioural data, co-expression of *ORMDL3* with *scSPT*[T51I] did not fully suppress the production of C18 SLs (Fig. 6F and G). These results provided compelling evidence that the elevation of SL synthesis correlates with the lethality and neurological phenotypes observed *in vivo*. In summary, our findings in *Drosophila* showed that excessive SL synthesis causes motor defects and

shortened lifespan, supporting that the phenotypes observed in the patients are indeed caused by the *SPTSSA* variants.

Discussion

Here, we have defined novel *SPTSSA* variants and linked them for the first time to human disease, specifically complex HSP. HSPs represent a genetically heterogeneous group of disorders characterized by progressive spasticity and weakness, particularly in the lower extremities. Complex HSPs often represent diffuse cortical dysfunction (e.g. seizures, ID and sensorineural hearing loss) along with somatic changes (e.g. port-wine stain), while uncomplicated ('pure') HSPs affect only motor pathways. We have presented three individuals who have either monoallelic *de novo* or biallelic inherited mutations in *SPTSSA*. These individuals have motor impairment and progressive lower extremity spasticity (consistent with the classification of HSP) as well as neurological findings, including cognitive impairment and hearing loss (consistent with the classification of 'complex' HSP).

Using biochemical and cell-based assays, we have shown that the *SPTSSA* variants cause loss of ORMDL regulation that leads to
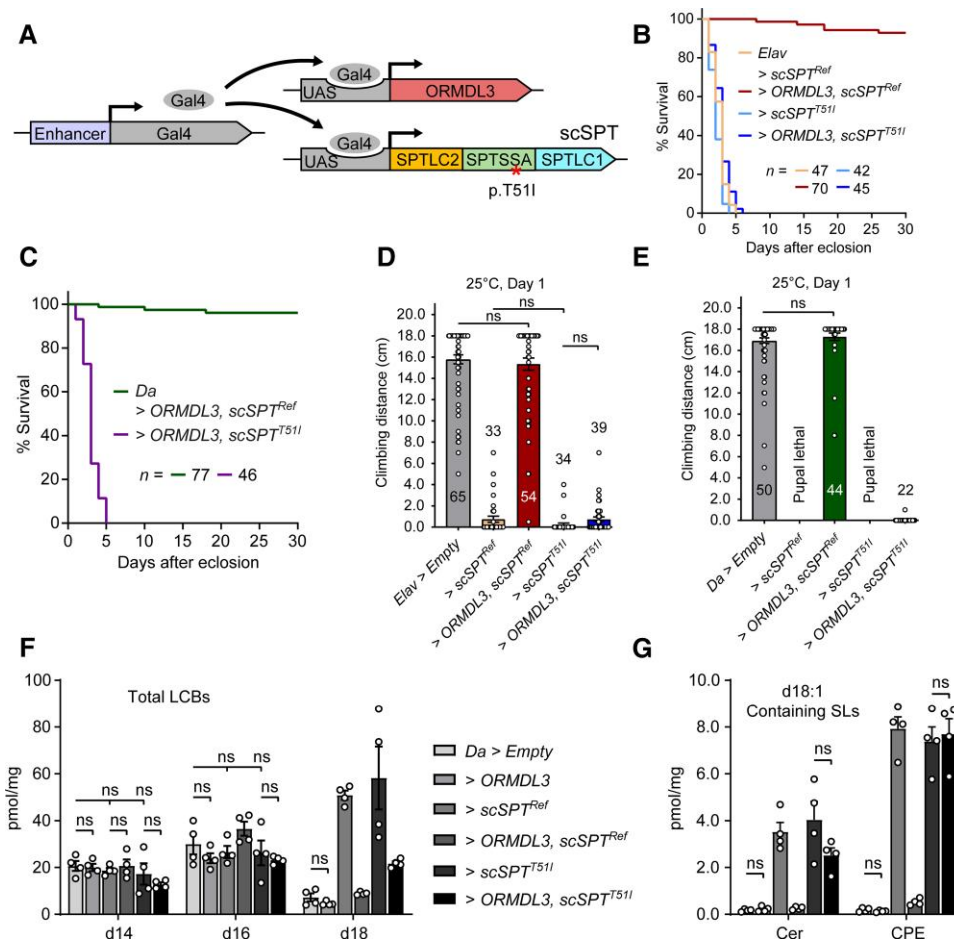
Figure 6 Increased SPT activity causes neurological defects in *Drosophila*. (**A**) Schematic of the constructs used in *Drosophila* that overexpresses human SPT and ORMDL3. (**B**) Neuronal overexpression of scSPT causes shortened lifespan. ORMDL3 expression rescues the lifespan in flies expressing WT scSPT (scSPTRef) but not in flies expressing the p.Thr51Ile scSPT variant (scSPTp.T51I). (**C**) Flies co-expressing ORMDL3 and scSPTp.T51I have a shortened lifespan when compared to those co-expressing ORMDL3 and scSPTRef. (**D**) Neuronal expression of scSPT causes severe climbing defects. ORMDL3 expression recovers the climbing capability in flies expressing scSPTRef but not those expressing scSPTp.T51I. The *elav>Empty* flies were tested to document the climbing capability of the proper control flies. (**E**) Flies co-expressing ORMDL3 and scSPTp.T51I exhibit severely compromised climbing capabilities when compared to flies co-expressing ORMDL3 and scSPTRef. The *da>Empty* flies were tested as controls. (**B–E**) *n* values are indicated in each panel. (**F**) Expression of scSPT causes elevated production of C18, but not C14 and C16 LCBs. Co-expression of ORMDL3 fully suppresses the C18 LCB production induced by scSPTRef, but only partially suppresses the C18 production induced by scSPTp.T51I. (**G**) Expression of scSPT causes production of C18 ceramide and C18 CPE, two complex SL species commonly observed in *Drosophila*. Data are presented as Kaplan–Meier curves and analysed using Gehan–Breslow–Wilcoxon test and log-rank test (**B** and **C**) or represented as mean ± SEM and analysed using unpaired Student's *t*-test (**D–G**). Unless indicated as not significant (ns), all differences were significant ($P < 0.05$).

inappropriately high SPT activity. Unrestrained SPT was evident from elevated SLs in serum and fibroblasts from the patients. In addition, we overexpressed human SPT in fruit flies and showed that it leads to excessive SL synthesis that causes severe motor defects and shortened lifespan, supporting the causal relationship between elevated SPT activity and some of the patient phenotypes. Moreover, while co-expression of human ORMDL3 rescued the phenotypes of flies expressing the WT human SPT, it failed to rescue flies expressing the mutant SPT, confirming that the SPTSSA[T51I] variant abrogates ORMDL regulation of SPT. In all, we identified *SPTSSA* as the latest gene to be associated with complex HSP, a genetically and clinically diverse group of neurological disorders.[43,44]

The first report of enhanced SPT activity resulting in neurodegenerative disease came from the study of the *stellar* mouse with an autosomal dominant eye-flecking phenotype.[39] Homozygous *stellar* mice developed early onset ataxia and died prematurely

(~10 weeks). Degenerating axons were observed by EM in these mice at 2 weeks of age. The variant was mapped to the *Sptssb* gene, encoding a structural and functional homolog of SPTSSA, and the SPTSSB[H56L] mutant caused elevated SPT activity and increased levels of SLs. At the time, the importance of the C-terminal domain of the SPTSS subunits in ORMDL-mediated regulation was not appreciated, but here we have shown that this histidine residue, highly conserved between SPTSSB (H56) and SPTSSA (H59), is critical for ORMDL regulation of SPT (Supplementary Figs 3A and 4). The SPTSSA H59 residue localizes to the C-terminal region affected by the 58fs frameshift variant and the C-terminal deletion mutant. The results from all these variants highlight the important role of the C-terminus of SPTSSA in ORMDL regulation.

Specific genetic alterations in *SPTSSA* affect ORMDL regulation to different degrees and manifest with variable severity of the

Table 2 Summary of the phenotypes of flies overexpressing scSPT and ORMDL3 in various tissues

	UAS-scSPT[Ref]	UAS-scSPT[Ref], UAS-ORMDL3	UAS-scSPT[T51I]	UAS-scSPT[T51I], UAS-ORMDL3
Da-Gal4 (ubiquitous)	Lethal (pupa)[a]	Viable, no motor defect	Lethal (pupa)	Short lifespan, motor defects
Act-Gal4 (ubiquitous)	Lethal (multi-phase)	Viable, no motor defect	Not tested	Not tested
Elav-Gal4 (neurons)	Short lifespan, motor defects	Phenotypes rescued	Short lifespan, motor defects	Phenotypes NOT rescued
Repo-Gal4 (glia)	Lethal (pupa)	Viable, no motor defect	Not tested	Not tested
Mef2-Gal4 (muscles)	Lethal (multi-phase)	Viable, no motor defect	Not tested	Not tested
SPARC-Gal4 (fat body)	Lethal (multi-phase)	Viable, no motor defect	Not tested	Not tested

For the genotypes that cause lethality, the lethality phases of the animals are indicated in the table.
[a]All experiments were carried out at 25°C.

associated complex HSP phenotype. The individuals with the *de novo* T51I variant, which renders SPT less responsive to ORMDL regulation than the SPTSSA[58fs] variant, had earlier onset of disease and more severe motor and cognitive deficits. The lower SL accumulation associated with the SPTSSA[58fs] variant and the fact that it was only deleterious in the homozygous state likely reflected, in part, that SPTSSA[58fs] was poorly expressed and thus that the majority of SPT in heterozygous individuals contains WT SPTSSA. In addition, ORMDL regulation was less severely impacted by the SPTSSA[58fs] variant than by the T51I variant. For example, silencing the ORMDLs increased *de novo* SLs 5- to 10-fold in *SPTSSA* KO cells expressing WT SPTSSA (Fig. 5D) but did not significantly change *de novo* SL synthesis in cells expressing SPTSSA[T51I], showing that ORMDL regulation was largely ablated by this mutation. In the case of *SPTSSA* KO cells expressing SPTSSA[58fs], *de novo* SLs increased 2- to 3-fold, indicating that, although significantly blunted, the ORMDLs partially regulated SPT containing SPTSSA[58fs]. Thus, the extent of loss of ORMDL regulation may predict clinical severity.

Though the individuals with the *de novo* T51I variant were more severely impacted clinically, there are common neurological features of the disorder, including developmental delay, progressive motor impairment, progressive lower extremity spasticity, and epileptiform activity or seizures. Brain MRI from the affected patients showed variable features, including cerebral/cerebellar atrophy, thin corpus callosum, and hyperintensity in the deep and periventricular white matter. Although abnormal SLs are associated with a number of leukodystrophies as well as multiple sclerosis,[45] the overall clinical picture, including the presence of epileptiform activity or seizures and cerebral/cerebellar atrophy, suggest a neuronal disorder rather than a white matter disorder (i.e. leukodystrophy).[46] The findings on magnetic resonance spectroscopy are limited but provide potentially valuable additional information. In addition to lactate peaks, Patient 2 showed a decrease in N-acetylaspartate, a marker of neuronal and axonal health, in both grey and white matter of the brain. It is difficult to draw conclusive statements from this single patient, but overall, the clinical and imaging findings point to an impact of the *SPTSSA* variants upon neuronal health during early childhood brain development.

Despite the evidence that this is a neuronal disorder, the neurological phenotypes may be secondary to myelination defects associated with the *SPTSSA* variants. During myelination, there is an increased rate of SL synthesis and maturation of oligodendrocytes coincides with alterations in expression of SPT subunits including SPTSSA and SPTSSB. Thus, the composition of the SPT complex undergoes changes during this developmental stage.[47] Under these conditions, the ORMDLs appear to be especially crucial for preventing the synthesis of potentially toxic intermediates, such as ceramides. For example, it has been shown that either deletion of

Ormdls (in the *Ormdl1/3* double KO mice) or overexpression of scSPT specifically in myelin-producing cells result in severe dysmyelination and neurological phenotypes in mice.[9] *Drosophila* wrapping glia perform similar functions as the myelin-forming Schwann cells and oligodendrocytes. The development of fly wrapping glia requires SLs[48,49] and selective expression of the scSPT in glial cells in flies is sufficient to induce lethality (Table 2). These studies point to the importance of deciphering precisely how elevated SL synthesis impacts myelination and disrupts brain development.

To address whether excessive SL leads to neurological sequelae, we successfully generated human SPT overexpressing fruit flies to model the consequences of elevated SPT activity and SL accumulation. We showed that excessive production of C18 SLs caused severe motor defects and a shortened lifespan in flies, similar to the neurodegenerative phenotypes in patients. Our data support a causative relationship between elevated SL synthesis and neurological phenotypes. However, the difference in chain lengths of human and fly sphingoid bases raises interesting questions. Further studies are needed to determine whether excessive SLs in general or specifically the presence of C18 SLs was responsible for the neurological damage in the fly model. However, previous studies have shown that accumulation of endogenous fly SLs is toxic.[50–53] Beyond diseases caused by unregulated SPT activity, SL accumulation has been observed in models for a number of neurological disorders including Parkinson's disease,[40,53,54] Gaucher disease,[55] Krabbe disease,[56] Infantile Neuroaxonal Dystrophy[52] and Friedreich's ataxia.[50,51] How dysregulated SL metabolism relates to these different pathological manifestations remains to be investigated.

Unregulated activity of SPT and excessive SL synthesis have been implicated in at least one other human neurological disease. A recent study of seven families identified four specific, dominantly-acting *SPTLC1* variants manifesting as juvenile ALS.[10] Similar to the *SPTSSA* variants described here, these mutations disrupted the normal homeostatic regulation of SPT by ORMDL, resulting in unregulated SPT activity and elevated levels of canonical SPT products. Altered CSF lipids have also been described in sporadic ALS,[57–60] suggesting a broader pathogenic role for disrupted SL metabolism in sporadic ALS.

It is not uncommon for distinct biochemical consequences of various mutations in SPT to result in different disease phenotypes. For example, previously described pathogenic variants in *SPTLC1* or *SPTLC2* that result in elevated deoxy-SLs cause sensory neuropathy, whereas variants in *SPTLC1* that result in excessive synthesis of canonical SLs cause early-onset ALS. Interestingly, the *SPTSSA* variants described here that similarly resulted in elevated canonical SLs caused neither peripheral neuropathy nor lower motor neuron

disease, but rather a complex form of HSP. This is supported by NCA that showed no abnormalities in the *SPTSSA* patients.

Understanding the biochemical consequences of the variants in SPT has important therapeutic implications. For example, in the case of the HSAN1 variants, the promiscuous utilization of alanine by SPT producing deoxy-SLs can be reduced by increasing the ratio of serine to alanine.[30,61] Thus, dietary serine supplementation is being tested for therapeutic benefit in these patients.[62] On the other hand, elevated serine exacerbates the overproduction of SLs associated with the *SPTLC1* juvenile ALS variants[10] and the *SPTSSA* variants described here (Fig. 5B). Thus serine supplementation is not a rational therapeutic strategy and may even be detrimental for these patients.

We do not yet understand why mutations in different subunits of SPT that similarly impact ORMDL regulation cause such distinct clinical presentations. In this regard, it is interesting that many of the early-onset ALS patients first presented with upper motor neuron weakness and some were initially diagnosed with HSP or cerebral palsy.[10] Of note, the patients presented here did not have evidence of lower motor neuron pathology on EMG/NCS as would be seen in ALS; however, the possibility of development of ALS features in the future cannot be excluded. Although both the *SPTLC1* ALS and *SPTSSA* HSP variants impair ORMDL regulation of SPT, there are important distinctions. As mentioned earlier, there are two isoforms of the activating small subunit (SPTSSA and SPTSSB) and two isoforms of the other catalytic subunit (SPTLC2 and SPTLC3), but a single isoform of SPTLC1. The physiological significance of the different SPT isozymes is not understood, but they have distinct acyl-CoA chain length substrate preferences that contribute to an array of sphingoid bases.[11,31,63] All SPT isozymes contain SPTLC1 and are thus dysregulated in the ALS patients, but in the HSP patients only the isozymes containing SPTSSA are affected. Moreover, the SPTSSB-containing isozymes, with intact ORMDL regulation, may be hyper-repressed due to excessive activity of the SPTSSA isozymes. The importance of these complexities needs to be further investigated.

In summary, we report the first three patients with disease-causing mutations in *SPTSSA*. Our evidence that SPTSSA[T51I] interferes with ORMDL regulation is supported by the recently solved structure of the SPT/ORMDL3 complex, in which Thr51 of SPTSSA directly contacts ORMDL3 (Fig. 1). Our data also implicate the C-terminal domain of SPTSSA, missing in the SPTSSA[58fs] mutant, in ORMDL regulation. It is worth noting that the C-terminal domain of SPTSSA was not visible in the cryo-EM structure of the SPT/ORMDL complex.[12,13] This suggests that the domain is flexible and may undergo conformational changes related to ORMDL regulation. It is likely that additional disease-causing *de novo* mutations in the SPTSS subunits will provide further insight into the regulation of SPT and inform therapeutic strategies for restoring SL homeostasis.

Acknowledgements

Funding

Competing interests

B.P.K. is an inventor on patents and patent applications filed by Mass General Brigham that describe genome engineering technologies. B.P.K. consults for Avectas Inc., EcoR1 capital and ElevateBio, and is an advisor to Acrigen Biosciences, Life Edit Therapeutics and Prime Medicines. S.S. has received consulting fees from GLG, Guidepoint (which connected to a client, Fortress Biotech), Novartis, ExpertConnect and Orchard Therapeutics. F.E. has received consulting fees for UptoDate, Prime Medical Education, bluebird bio, Takeda and SwanBio Therapeutics. All other authors declare no competing interests.

Supplementary material

Supplementary material is available at *Brain* online.

Appendix 1
Undiagnosed Disease Network Consortia members

Mercedes E. Alejandro, Mahshid S. Azamian, Carlos A. Bacino, Ashok Balasubramanyam, Lindsay C. Burrage, Hsiao-Tuan Chao, Gary D. Clark, William J. Craigen, Hongzheng Dai, Shweta U. Dhar, Lisa T. Emrick, Alica M. Goldman, Neil A. Hanchard, Fariha Jamal, Lefkothea Karaviti, Seema R. Lalani, Brendan H. Lee, Richard A. Lewis, Ronit Marom, Paolo M. Moretti, David R. Murdock, Sarah K. Nicholas, James P. Orengo, Jennifer E. Posey, Lorraine Potocki, Jill A. Rosenfeld, Susan L. Samson, Daryl A. Scott, Alyssa A. Tran, Tiphanie P. Vogel, Michael F. Wangler, Shinya Yamamoto, Christine M. Eng, Pengfei Liu, Patricia A. Ward, Edward Behrens, Matthew Deardorff, Marni Falk, Kelly Hassey, Kathleen Sullivan, Adeline Vanderver, David B. Goldstein, Heidi Cope, Allyn McConkie-Rosell, Kelly Schoch, Vandana Shashi, Edward C. Smith, Rebecca C. Spillmann, Jennifer A. Sullivan, Queenie K.-G. Tan, Nicole M. Walley, Pankaj B. Agrawal, Alan H. Beggs, Gerard T. Berry, Lauren C. Briere, Laurel A. Cobban, Matthew Coggins, Cynthia M. Cooper, Elizabeth L. Fieg, Frances High, Ingrid A. Holm, Susan Korrick, Joel B. Krier, Sharyn A. Lincoln, Joseph Loscalzo, Richard L. Maas, Calum A. MacRae, J. Carl Pallais, Deepak A. Rao, Lance H. Rodan, Edwin K. Silverman, Joan M. Stoler, David A. Sweetser, Melissa Walker, Chris A. Walsh, Cecilia Esteves, Emily G. Kelley, Isaac S. Kohane, Kimberly LeBlanc, Alexa T. McCray, Anna Nagy, Surendra Dasari, Brendan C. Lanpher, Ian R. Lanza, Eva Morava, Devin Oglesbee, Guney Bademci, Deborah Barbouth, Stephanie Bivona, Olveen Carrasquillo, Ta Chen Peter Chang, Irman Forghani, Alana Grajewski, Rosario Isasi, Byron Lam, Roy Levitt, Xue Zhong Liu, Jacob McCauley, Ralph Sacco, Mario Saporta, Judy Schaechter, Mustafa Tekin, Fred Telischi, Willa Thorson, Stephan Zuchner,

Heather A. Colley, Jyoti G. Dayal, David J. Eckstein, Laurie C. Findley, Donna M. Krasnewich, Laura A. Mamounas, Teri A. Manolio, John J. Mulvihill, Grace L. LaMoure, Madison P. Goldrich, Tiina K. Urv, Argenia L. Doss, Maria T. Acosta, Carsten Bonnenmann, Precilla D'Souza, David D. Draper, Carlos Ferreira, Rena A. Godfrey, Catherine A. Groden, Ellen F. Macnamara, Valerie V. Maduro, Thomas C. Markello, Avi Nath, Donna Novacic, Barbara N. Pusey, Camilo Toro, Colleen E. Wahl, Eva Baker, Elizabeth A. Burke, David R. Adams, William A. Gahl, May Christine V. Malicdan, Cynthia J. Tifft, Lynne A. Wolfe, John Yang, Bradley Power, Bernadette Gochuico, Laryssa Huryn, Lea Latham, Joie Davis, Deborah Mosbrook-Davis, Francis Rossignol, Ben Solomon, John MacDowall, Audrey Thurm, Wadih Zein, Muhammad Yousef, Margaret Adam, Laura Amendola, Michael Bamshad, Anita Beck, Jimmy Bennett, Beverly Berg-Rood, Elizabeth Blue, Brenna Boyd, Peter Byers, Sirisak Chanprasert, Michael Cunningham, Katrina Dipple, Daniel Doherty, Dawn Earl, Ian Glass, Katie Golden-Grant, Sihoun Hahn, Anne Hing, Fuki M. Hisama, Martha Horike-Pyne, Gail P. Jarvik, Jeffrey Jarvik, Suman Jayadev, Christina Lam, Kenneth Maravilla, Heather Mefford, J. Lawrence Merritt, Ghayda Mirzaa, Deborah Nickerson, Wendy Raskind, Natalie Rosenwasser, C. Ron Scott, Angela Sun, Virginia Sybert, Stephanie Wallace, Mark Wener, Tara Wenger, Euan A. Ashley, Gill Bejerano, Jonathan A. Bernstein, Devon Bonner, Terra R. Coakley, Liliana Fernandez, Paul G. Fisher, Laure Fresard, Jason Hom, Yong Huang, Jennefer N. Kohler, Elijah Kravets, Marta M. Majcherska, Beth A. Martin, Shruti Marwaha, Colleen E. McCormack, Archana N. Raja, Chloe M. Reuter, Maura Ruzhnikov, Jacinda B. Sampson, Kevin S. Smith, Shirley Sutton, Holly K. Tabor, Brianna M. Tucker, Matthew T. Wheeler, Diane B. Zastrow, Chunli Zhao, William E. Byrd, Andrew B. Crouse, Matthew Might, Mariko Nakano-Okuno, Jordan Whitlock, Gabrielle Brown, Manish J. Butte, Esteban C. Dell'Angelica, Naghmeh Dorrani, Emilie D. Douine, Brent L. Fogel, Irma Gutierrez, Alden Huang, Deborah Krakow, Hane Lee, Sandra K. Loo, Bryan C. Mak, Martin G. Martin, Julian A. Martínez-Agosto, Elisabeth McGee, Stanley F. Nelson, Shirley Nieves-Rodriguez, Christina G. S. Palmer, Jeanette C. Papp, Neil H. Parker, Genecee Renteria, Rebecca H. Signer, Janet S. Sinsheimer, Jijun Wan, Lee-kai Wang, Katherine Wesseling Perry, Jeremy D. Woods, Justin Alvey, Ashley Andrews, Jim Bale, John Bohnsack, Lorenzo Botto, John Carey, Laura Pace, Nicola Longo, Gabor Marth, Paolo Moretti, Aaron Quinlan, Matt Velinder, Dave Viskochi, Pinar Bayrak-Toydemir, Rong Mao, Monte Westerfield, Anna Bican, Elly Brokamp, Laura Duncan, Rizwan Hamid, Jennifer Kennedy, Mary Kozuira, John H. Newman, John A. PhillipsIII, Lynette Rives, Amy K. Robertson, Emily Solem, Joy D. Cogan, F. Sessions Cole, Nichole Hayes, Dana Kiley, Kathy Sisco, Jennifer Wambach, Daniel Wegner, Dustin Baldridge, Stephen Pak, Timothy Schedl, Jimann Shin, and Lilianna Solnica-Krezel.

References

1. Hannun YA, Obeid LM. Sphingolipids and their metabolism in physiology and disease. *Nat Rev Mol Cell Biol*. 2018;19:175-191.
2. Olsen ASB, Faergeman NJ. Sphingolipids: Membrane microdomains in brain development, function and neurological diseases. *Open Biol*. 2017;7:170069
3. Dunn TM, Tifft CJ, Proia RL. A perilous path: The inborn errors of sphingolipid metabolism. *J Lipid Res*. 2019;60:475-483.
4. Kolter T, Sandhoff K. Sphingolipid metabolism diseases. *Biochim Biophys Acta*. 2006;1758:2057-2079.
5. Hanada K. Serine palmitoyltransferase, a key enzyme of sphingolipid metabolism. *Biochim Biophys Acta*. 2003;1632:16-30.
6. Harrison PJ, Dunn TM, Campopiano DJ. Sphingolipid biosynthesis in man and microbes. *Nat Prod Rep*. 2018;35:921-954.
7. Merrill AH Jr, Nixon DW, Williams RD. Activities of serine palmitoyltransferase (3-ketosphinganine synthase) in microsomes from different rat tissues. *J Lipid Res*. 1985;26:617-622.
8. Breslow DK. Sphingolipid homeostasis in the endoplasmic reticulum and beyond. *Cold Spring Harb Perspect Biol*. 2013;5:a013326.
9. Clarke BA, Majumder S, Zhu H, *et al*. The ORMDL genes regulate the sphingolipid synthesis pathway to ensure proper myelination and neurologic function in mice. *Elife*. 2019;8:e51067.
10. Mohassel P, Donkervoort S, Lone MA, *et al*. Childhood amyotrophic lateral sclerosis caused by excess sphingolipid synthesis. *Nat Med*. 2021;27:1197-1204.
11. Han G, Gupta SD, Gable K, *et al*. Identification of small subunits of mammalian serine palmitoyltransferase that confer distinct acyl-CoA substrate specificities. *Proc Natl Acad Sci U S A*. 2009; 106:8186-8191.
12. Li S, Xie T, Liu P, Wang L, Gong X. Structural insights into the assembly and substrate selectivity of human SPT-ORMDL3 complex. *Nat Struct Mol Biol*. 2021;28:249-257.
13. Wang Y, Niu Y, Zhang Z, *et al*. Structural insights into the regulation of human serine palmitoyltransferase complexes. *Nat Struct Mol Biol*. 2021;28:240-248.
14. Wattenberg BW. Kicking off sphingolipid biosynthesis: Structures of the serine palmitoyltransferase complex. *Nat Struct Mol Biol*. 2021;28:229-231.
15. Breslow DK, Collins SR, Bodenmiller B, *et al*. ORM family proteins mediate sphingolipid homeostasis. *Nature*. 2010;463: 1048-1053.
16. Davis D, Kannan M, Wattenberg B. ORM/ORMDL proteins: Gate guardians and master regulators. *Adv Biol Regul*. 2018;70:3-18.
17. Han S, Lone MA, Schneiter R, Chang A. ORM1 and ORM2 are conserved endoplasmic reticulum membrane proteins regulating lipid homeostasis and protein quality control. *Proc Natl Acad Sci U S A*. 2010;107:5851-5856.
18. Dawkins JL, Hulme DJ, Brahmbhatt SB, Auer-Grumbach M, Nicholson GA. Mutations in SPTLC1, encoding serine palmitoyltransferase, long chain base subunit-1, cause hereditary sensory neuropathy type I. *Nat Genet*. 2001;27:309-312.
19. Nicholson GA. SPTLC1-related Hereditary sensory neuropathy. In: Adam MP, Everman DB, Mirzaa GM, *et al*, eds. *GeneReviews®*. University of Washington; 1993-2023.
20. Eichler FS, Hornemann T, McCampbell A, *et al*. Overexpression of the wild-type SPT1 subunit lowers desoxysphingolipid levels and rescues the phenotype of HSAN1. *J Neurosci*. 2009;29: 14646-14651.
21. Rotthier A, Auer-Grumbach M, Janssens K, *et al*. Mutations in the SPTLC2 subunit of serine palmitoyltransferase cause hereditary sensory and autonomic neuropathy type I. *Am J Hum Genet*. 2010;87:513-522.
22. Penno A, Reilly MM, Houlden H, *et al*. Hereditary sensory neuropathy type 1 is caused by the accumulation of two neurotoxic sphingolipids. *J Biol Chem*. 2010;285:11178-11187.
23. Gantner ML, Eade K, Wallace M, *et al*. Serine and lipid metabolism in macular disease and peripheral neuropathy. *N Engl J Med*. 2019;381:1422-1433.
24. Johnson JO, Chia R, Miller DE, *et al*. Association of Variants in the SPTLC1 Gene With Juvenile Amyotrophic Lateral Sclerosis. *JAMA Neurol*. 2021;78:1236-1248.
25. Gupta SD, Gable K, Alexaki A, *et al*. Expression of the ORMDLS, modulators of serine palmitoyltransferase, is regulated by sphingolipids in mammalian cells. *J Biol Chem*. 2015;290:90-98.

26. Mohassel P, Liewluck T, Hu Y, et al. Dominant collagen XII mutations cause a distal myopathy. Ann Clin Transl Neurol. 2019;6: 1980-1988.

27. Harnish JM, Deal SL, Chao HT, Wangler MF, Yamamoto S. In vivo functional study of disease-associated rare human variants using Drosophila. J Vis Exp. 2019;150:10.3791/59658.

28. Bischof J, Bjorklund M, Furger E, Schertel C, Taipale J, Basler K. A versatile platform for creating a comprehensive UAS-ORFeome library in Drosophila. Development. 2013;140:2434-2442.

29. Venken KJ, He Y, Hoskins RA, Bellen HJ. P[acman]: A BAC transgenic platform for targeted insertion of large DNA fragments in D. Melanogaster. Science. 2006:314:1747-1751.

30. Gable K, Gupta SD, Han G, Niranjanakumari S, Harmon JM, Dunn TM. A disease-causing mutation in the active site of serine palmitoyltransferase causes catalytic promiscuity. J Biol Chem. 2010;285:22846-22852.

31. Harmon JM, Bacikova D, Gable K, et al. Topological and functional characterization of the ssSPTs, small activating subunits of serine palmitoyltransferase. J Biol Chem. 2013;288:10144-10153.

32. Davis DL, Gable K, Suemitsu J, Dunn TM, Wattenberg BW. The ORMDL/ORM-serine palmitoyltransferase (SPT) complex is directly regulated by ceramide: Reconstitution of SPT regulation in isolated membranes. J Biol Chem. 2019;294:5146-5156.

33. Livak KJ, Schmittgen TD. Analysis of relative gene expression data using real-time quantitative PCR and the 2(-Delta Delta C(T)) method. Methods. 2001;25:402-408.

34. Lu S, Hernan R, Marcogliese PC, et al. Loss-of-function variants in TIAM1 are associated with developmental delay, intellectual disability, and seizures. Am J Hum Genet. 2022;109:571-586.

35. Parthibane V, Lin J, Acharya D, et al. SSSPTA Is essential for serine palmitoyltransferase function during development and hematopoiesis. J Biol Chem. 2021;296:100491.

36. Karczewski KJ, Francioli LC, Tiao G, et al. The mutational constraint spectrum quantified from variation in 141,456 humans. Nature. 2020;581:434-443.

37. Siow D, Sunkara M, Dunn TM, Morris AJ, Wattenberg B. ORMDL/ Serine palmitoyltransferase stoichiometry determines effects of ORMDL3 expression on sphingolipid biosynthesis. J Lipid Res. 2015;56:898-908.

38. Siow DL, Wattenberg BW. Mammalian ORMDL proteins mediate the feedback response in ceramide biosynthesis. J Biol Chem. 2012;287:40198-40204.

39. Zhao L, Spassieva S, Gable K, et al. Elevation of 20-carbon long chain bases due to a mutation in serine palmitoyltransferase small subunit b results in neurodegeneration. Proc Natl Acad Sci U S A. 2015;112:12962-12967.

40. Lin G, Wang L, Marcogliese PC, Bellen HJ. Sphingolipids in the pathogenesis of Parkinson's disease and parkinsonism. Trends Endocrinol Metab. 2019;30:106-117.

41. Ma M, Moulton MJ, Lu S, Bellen HJ. 'Fly-ing' from rare to common neurodegenerative disease mechanisms. Trends Genet. 2022;38: 972-984.

42. Fyrst H, Herr DR, Harris GL, Saba JD. Characterization of free endogenous C14 and C16 sphingoid bases from Drosophila melanogaster. J Lipid Res. 2004;45:54-62.

43. Blackstone C. Hereditary spastic paraplegia. Handb Clin Neurol. 2018;148:633-652.

44. Yahia A, Stevanin G. The history of gene hunting in hereditary spinocerebellar degeneration: Lessons from the past and future perspectives. Front Genet. 2021;12:638730.

45. Giussani P, Prinetti A, Tringali C. The role of sphingolipids in myelination and myelin stability and their involvement in childhood and adult demyelinating disorders. J Neurochem. 2021;156:403-414.

46. Schiffmann R, van der Knaap MS. Invited article: An MRI-based approach to the diagnosis of white matter disorders. Neurology. 2009;72:750-759.

47. Davis DL, Mahawar U, Pope VS, Allegood J, Sato-Bigbee C, Wattenberg BW. Dynamics of sphingolipids and the serine palmitoyltransferase complex in rat oligodendrocytes during myelination. J Lipid Res. 2020;61:505-522.

48. Kottmeier R, Bittern J, Schoofs A, et al. Wrapping glia regulates neuronal signaling speed and precision in the peripheral nervous system of Drosophila. Nat Commun. 2020;11:4491.

49. Yildirim K, Petri J, Kottmeier R, Klambt C. Drosophila glia: Few cell types and many conserved functions. Glia. 2019;67:5-26.

50. Chen K, Ho TS, Lin G, Tan KL, Rasband MN, Bellen HJ. Loss of frataxin activates the iron/sphingolipid/PDK1/Mef2 pathway in mammals. Elife. 2016;5:e20732.

51. Chen K, Lin G, Haelterman NA, et al. Loss of frataxin induces iron toxicity, sphingolipid synthesis, and Pdk1/Mef2 activation, leading to neurodegeneration. Elife. 2016;5:e16043.

52. Lin G, Lee PT, Chen K, et al. Phospholipase PLA2G6, a parkinsonism-associated gene, affects Vps26 and Vps35, retromer function, and ceramide levels, similar to alpha-synuclein gain. Cell Metab. 2018;28:605-618.e6.

53. Vos M, Dulovic-Mahlow M, Mandik F, et al. Ceramide accumulation induces mitophagy and impairs beta-oxidation in PINK1 deficiency. Proc Natl Acad Sci U S A. 2021;118:e2025347118.

54. Custodia A, Aramburu-Nunez M, Correa-Paz C, et al. Ceramide metabolism and Parkinson's disease-therapeutic targets. Biomolecules. 2021;11(7):945.

55. Kinghorn KJ, Gronke S, Castillo-Quan JI, et al. A Drosophila model of neuronopathic gaucher disease demonstrates lysosomal-autophagic defects and altered mTOR signalling and is functionally rescued by rapamycin. J Neurosci. 2016;36: 11654-11670.

56. White AB, Givogri MI, Lopez-Rosas A, et al. Psychosine accumulates in membrane microdomains in the brain of krabbe patients, disrupting the raft architecture. J Neurosci. 2009;29: 6068-6077.

57. Gutner UA, Shupik MA, Maloshitskaya OA, et al. Changes in the metabolism of sphingoid bases in the brain and spinal cord of transgenic FUS(1-359) mice, a model of amyotrophic lateral sclerosis. Biochemistry (Mosc). 2019;84:1166-1176.

58. Rapport MM. Implications of altered brain ganglioside profiles in amyotrophic lateral sclerosis (ALS). Acta Neurobiol Exp (Wars). 1990;50:505-513.

59. Sen NE, Arsovic A, Meierhofer D, et al. In human and mouse spino-cerebellar tissue, ataxin-2 expansion affects ceramide-sphingomyelin metabolism. Int J Mol Sci. 2019;20:5854.

60. Trostchansky A. Overview of lipid biomarkers in amyotrophic lateral sclerosis (ALS). Adv Exp Med Biol. 2019;1161:233-241.

61. Garofalo K, Penno A, Schmidt BP, et al. Oral L-serine supplementation reduces production of neurotoxic deoxysphingolipids in mice and humans with hereditary sensory autonomic neuropathy type 1. J Clin Invest. 2011;121: 4735-4745.

62. Fridman V, Suriyanarayanan S, Novak P, et al. Randomized trial of l-serine in patients with hereditary sensory and autonomic neuropathy type 1. Neurology. 2019;92:e359-e370.

63. Lone MA, Hulsmeier AJ, Saied EM, et al. Subunit composition of the mammalian serine-palmitoyltransferase defines the spectrum of straight and methyl-branched long-chain bases. Proc Natl Acad Sci U S A. 2020;117:15591-15598.